TIMP-1 attenuates the development of cutaneous inflammation-induced evoked and ongoing pain through receptor-mediated cell signaling

Knight, B.E.[3], Kozlowski, N.,[1] Havelin, J.[7, 8], King T.[6, 7, 8], Crocker, S.J.[3, 5], Young, E.E.[1, 2, 4, 5], Baumbauer, K.M.[1, 2, 3, 5]

[1]School of Nursing, University of Connecticut, Storrs, CT, USA
[2]The Center for Advancement in Managing Pain, School of Nursing, University of Connecticut, Storrs, CT, USA
[3]Department of Neuroscience, UConn Health, Farmington, CT, USA
[4]Genetics and Genome Sciences, UConn Health, Farmington, CT, USA
[5]Institute for Systems Genomics, UConn Health, Farmington, CT, USA
[6]College of Osteopathic Medicine, University of New England, Biddeford, ME, USA
[7]Center for Excellence in the Neurosciences, University of New England, Biddeford, ME, USA
[8]Graduate School of Biomedical Science and Engineering, University of Maine, Orono, ME, USA

Direct correspondence to:

Kyle M. Baumbauer Ph.D.
Assistant Professor
University of Connecticut School of Nursing
Center for Advancements in Managing Pain
Storrs Hall, Room 308
231 Glenbrook Road, Unit 4026
Storrs, Connecticut 06269
Phone: (860) 486-0913
E mail: kyle.baumbauer@uconn.edu

ABSTRACT

Unresolved inflammation is a significant predictor for developing chronic pain, and targeting the mechanisms underlying inflammation offers opportunities for therapeutic intervention. During inflammation, matrix metalloproteinase (MMP) activity contributes to tissue remodeling and inflammatory signaling through proteolytic maturation of cytokines. MMP activity is regulated by tissue inhibitors of metalloproteinases (TIMPs) 1-4. TIMP-1 and -2 have known roles in pain, but only in the context of MMP inhibition. However, TIMP-1 also has receptor-mediated cell signaling functions that are not well understood. Here, we examined how TIMP-1-dependent cell signaling impacted inflammatory hypersensitivity and ongoing pain. We found that hindpaw injection of complete Freund's adjuvant (CFA) increased keratinocyte-derived TIMP-1 that peaked 3 days following inflammation, when mechanical hypersensitivity began to emerge in WT mice. These data suggest that TIMP-1 expression inhibits the development of inflammatory hypersensitivity. To examine this possibility, we injected TIMP-1 knockout (T1KO) mice with a diluted CFA mixture to examine how subtle cutaneous inflammation affected behavioral hypersensitivity. T1KO mice exhibited rapid onset thermal and mechanical hypersensitivity at the site of inflammation that was absent or attenuated in WT controls. We also found that T1KO mice exhibited hypersensitivity in adjacent tissues innervated by different sets of afferents, and skin contralateral to the site of inflammation. Replacement of recombinant murine (rm)TIMP-1 alleviated hypersensitivity when administered at the site and time of inflammation. To examine the MMP-dependent and -independent mechanisms of rmTIMP-1, T1KO mice were administered full-length rmTIMP-1, the N-terminal region (TIMP-1(N)) with MMP-inhibitory properties, or the C-terminal region (TIMP-1(C)) that retains receptor signaling function. Each of the peptides prevented inflammatory hypersensitivity, suggesting that rmTIMP-1 acts through mechanisms that

also include receptor-mediated cell signaling. We also found that hypersensitivity was neither due to genotype-specific differences in MMP-9 activity or expression, nor to differences in cytokine expression. Finally, to evaluate the potential clinical utility of TIMP-1, we administered rmTIMP-1 to WT mice and found that rmTIMP-1 prevented clonidine-induced conditioned place preference (e.g., ongoing pain) and inflammatory mechanical hypersensitivity. Collectively, our data suggest a novel role for TIMP-1 in the attenuation of inflammatory pain that occurs through previously uncharacterized cell signaling mechanisms.

Key words: Pain; thermal hyperalgesia; mechanical hypersensitivity; CD63; Ongoing Pain; Matrix metalloproteinase; Conditioned place preference

ACKNOWLEDGEMENTS

Research was supported by the Rita Allen Foundation (KMB), National Institutes of Health grants R03NS096454 (KMB), 1R21NS104789 (KMB), and National MS Society grant RG-1802-30211(SJC).

We would like to thank Ms. Nicole Glidden and Ms. Jessica Yasko for their technical assistance.

INTRODUCTION

Tissue inhibitors of matrix metalloproteinases (TIMPs) and matrix metalloproteinases (MMPs) are released during tissue damage to facilitate tissue remodeling through degradation and reorganization of the extracellular matrix (ECM) (Gardner and Ghorpade, 2003; Nagase et al., 2006; Ries, 2014). During this process MMPs also engage an inflammatory response through proteolytic maturation of cytokines, and both of these activities is regulated through a 1:1 stoichiometric interaction with one of four tissue inhibitors of metalloproteinases (TIMP-1, -2, -3, -4) (Huang et al., 2011). The interaction between MMPs and TIMPs is tightly controlled, but research has shown that during tissue damage, dysregulation in the balance of MMPs and TIMP function can lead to pathological conditions such as arthritis, multiple sclerosis, Parkinson's Disease, cancer, and even chronic pain (Nakagawa et al., 1994; Nagase et al., 1999; Kouwenhoven et al., 2001; Yang et al., 2002; Brew and Nagase, 2010). Studies examining the role of MMPs in pain specifically have shown that increased MMP-2 and -9 activity contribute to increased pain-related behavior in response to injury that are reversed by MMP antagonism (Kawasaki et al., 2008; Ji et al., 2009; Li et al., 2016; Remacle et al., 2018). These findings contributed, in part, to the development of several small molecule drugs that directly target and inhibit MMP activity. However, more than 50 clinical trials examining the efficacy of these drugs were discontinued due to the emergence of adverse events, including musculoskeletal pain (Cathcart and Cao, 2015; Martinho et al., 2016). While these trials indicated that specific targeting of MMP activity alone was not an effective strategy for pain treatment, they do suggest that additional mechanisms related to MMP activity may contribute to pain and its inhibition, a conclusion drawn from the very research that spawned the development of the MMP inhibitors; that endogenous inhibitors of MMP activity, such as TIMP-1 and -2 decrease pain-related behavior.

TIMP-1 has been best characterized as an endogenous inhibitor of MMP activity. Indeed, TIMP-1 regulates 14 of the 24 known MMPs (Baker et al., 2002; Gardner and Ghorpade, 2003; Nagase et al., 2006; Kawasaki et al., 2008), and has been shown to prevent the development of mechanical and thermal hypersensitivity following nerve damage (Kawasaki et al., 2008; Martinho et al., 2016). However, this identified role was characterized purely in the context of MMP inhibition. Interestingly, the structure of the protein allows it to function outside of its well-characterized role as MMP-inhibitor, an effect that is produced by binding of its N-terminal domain to MMPs. There is now mounting evidence that the C-terminal domain binds to membrane bound receptors, including CD63. Binding of TIMP-1 to CD63 engages intracellular signaling events that allow TIMP-1 to act as a trophic factor in the initiation of cell migration and differentiation (Gardner and Ghorpade, 2003; Jourquin et al., 2005; Thorne et al., 2009; Moore and Crocker, 2012; Claycomb et al., 2013).

Because TIMP-1 and MMPs can be up-regulated in concert with one another during tissue damage and repair, such as peripheral nerve injury (Parkitna et al., 2006; Huang et al., 2011; Kim et al., 2012; Yokose et al., 2012), it is difficult to disentangle how TIMP-1 regulates of tissue remodeling/repair and pain independent of one another.

Inflammation is a core component of the nerve injury process, and, in general, is a significant predictor of pain chronicity (Kehlet et al., 2006). Therefore, we used a model of cutaneous inflammation to examine the effects of TIMP-1 signaling on pain in the absence of frank tissue damage. We found that hindpaw injection of complete Freund's adjuvant (CFA) induced TIMP-1 expression in keratinocytes prior to the emergence of hypersensitivity in wildtype (WT) mice, suggesting that the release of TIMP-1 at the site of inflammation inhibited development of hypersensitivity. Supporting this conclusion, we found that TIMP-1 knockout (T1KO) mice

exhibited robust hypersensitivity local and distal to the site of inflammation that was prevented with the administration of recombinant murine (rm)TIMP-1 and the individual N- and C-terminal constructs at the time of CFA-injection. This result suggests that cell-signaling mechanisms may also contribute to the antinociceptive effects of TIMP-1. In addition, inflammation in WT and T1KO mice did not result in the activation or expression of cutaneous MMP-9 or cytokines in a genotype-specific manner. Finally, we found that administration of rmTIMP-1 prevented ongoing inflammatory pain and evoked mechanical sensitivity in WT mice. Collectively, our data suggests that TIMP-1 regulates the allogenic properties of inflammation and that TIMP-1 may be a target for improving pain management.

MATERIALS AND METHODS

Animals: Experiments were conducted using 8-12-week-old (20-30 g) male WT (C57BL/6; Jackson Laboratories, Bar Harbor, ME) and T1KO mice that were group housed, and maintained in a temperature-controlled environment on a 12 hr light-dark cycle with free access to food and water. TIMP-1 knockout (T1KO) mice (Lee et al., 2005) were backcrossed onto a C57BL/6 background for greater than 13 successive generations and bred in-house as a homozygous line (Crocker et al., 2006). All studies were approved by the UConn Health Institutional Animal Care and Use Committee and treated in accordance with published NIH standards.

Complete Freund's Adjuvant (CFA): To produce an acute, local inflammatory response, we subcutaneously (s.c.) injected the right hindpaw of mice with emulsified (50% in 10 μL) CFA (Sigma, St. Louis, MO). To assess primary hypersensitivity (i.e. at the site of inflammation) we administered CFA into the glabrous skin or ventral surface of the right hind paw. Conversely, secondary hypersensitivity was assessed in skin that was adjacent or contralateral to the site of inflammation. All samples were compared to naïve controls because in a pilot experiment we

found that vehicle injection alone caused increased sensitivity in T1KO mice (Figure 1). While this result is interesting and suggests that subtle perturbations cause robust alterations in sensory thresholds, adding saline-treated mice confounds our ability to examine the effects of inflammation. Therefore, to interpret the effects of inflammation *per se*, naïve mice were used as comparison controls. The literature is also mixed on the use of vehicle controls in experiments using CFA, and our experiments are in line with previously published work (Allchorne et al., 2005; Jankowski et al., 2012; Imbe and Kimura, 2017).

Recombinant Murine TIMP-1 Administration: WT and T1KO mice received injections (s.c.) of recombinant murine (rm) TIMP-1 (10 ng/μL, 10 μL; R&D Systems; Minneapolis, MN) immediately following CFA injection (10 μL) into the ipsilateral hindpaw. In subsequent experiments, T1KO mice received equimolar concentrations of the truncated C-terminus peptide (TIMP-1(C); 6.3kDa; Peptide 2.0 Inc., Chantilly, VA) that retains cell signaling function or the truncated N-terminus peptide (TIMP-1(N); 20 kDa; Abcam, Cambridge, UK) that retains MMP-inhibitory function and no cell-signaling ability, immediately following CFA injection.

von Frey testing: All mice were place into transparent Plexiglas chambers (radius = 32 mm, height = 108 mm) on an elevated mesh screen and were allowed to acclimate for a minimum of 1 hour before testing. To assess mechanical sensitivity, the plantar surface of the right hind paw was stimulated using von Frey filaments using the up-down method described by (Dixon, 1980). Nocifensive responses were counted as robust flexion responses, paw shaking, or paw licking and subtracted from individual baseline threshold to account for inter-subject variability. Data are presented as paw withdrawal thresholds (PWT; in grams).

Thermal hyperalgesia: Thermal hyperalgesia to radiant heat was assessed using a Hargreaves apparatus (Harvard Apparatus; Holliston, MA) (Hargreaves et al., 1988). Briefly, all mice were

placed in transparent Plexiglas chambers (radius = 32 mm, height= 108 mm) on top of a framed glass panel and were allowed to acclimate for a minimum of 1 hour before testing. Following the acclimation period, an infrared (IR) beam was aimed at the plantar surface of both hind paws. The intensity of the IR beam was chosen to produce average baseline paw withdrawal latency (PWL) of 15-20 seconds. Stimuli were presented 5 times in an alternating fashion between each hind paw with 5 minute intervals between successive stimulus exposures. PWLs collected from each paw were then averaged and analyzed. A 30 seconds exposure cutoff was employed to prevent tissue damage.

Conditioned Place Preference (CPP): CPP was used to assess ongoing pain in WT mice. A 3-day single trial protocol was used. On day 1, all mice freely explored a 3-chamber CPP box for 15 minutes prior to injection with CFA or saline. Preconditioning (baseline) behavior was analyzed using automated software (ANYMAZE, Stoelting) to ensure there were no baseline differences in the time spent in any of the chambers. On day 2 (conditioning day), all mice received an intrathecal (i.t.) injection of saline (5 μL volume) under isofluorane anesthesia and upon waking (within 2 min) were confined into the pre-assigned pairing chamber for 30 min. They were then returned to their home-cages for 4 hours. All mice then received an intrathecal (i.t.) injection of clonidine (2 μg/uL; 5 μL volume) through lumbar puncture and upon waking were confined to the opposite pairing chamber for 30 min. Vehicle and clonidine paired chambers were randomly assigned and counterbalanced between animals. On day 3 (test day), mice were returned to the CPP apparatus and allowed to freely explore all chambers across 15 min. The total time spent in each chamber was assessed using automated software (ANYMAZE). Conditioning day was 20-24 hours following CFA injection as previous research indicates ongoing pain is observed at this time-point

(Okun et al, He et al). A total of 17 mice were used, 8 were treated with rTIMP-1 and 9 with vehicle.

Tissue collection: Mice were anesthetized with a lethal dose of ketamine and xylazine mixture (90/10 mg/kg, respectively), intracardially perfused with ice cold 0.9% saline, prior to the dissection of ipsilateral hairy skin, L2 -L3 DRG, and L2 -L3 spinal cord segments. Tissues were collected following the completion of behavior or at designated time-points for molecular analysis.

Enzyme-linked immunosorbent assay (ELISA): Protein was extracted through homogenization in ice-cold RIPA buffer/protease inhibitor cocktail and spun for 20 min at 4°C at 18,000 rcf. Each sample's total protein concentration was determined using Pierce BCA Protein Assay Kit (ThermoFisher Scientific, Waltham, MA). The following ELISAs, TIMP-1 (R&D Systems, Minneapolis, MN), MMP-9 (R&D Systems; Minneapolis, MN), IL-6 (Invitrogen Carlsbad, CA), TNF-α (ThermoFisher Scientific, Waltham, MA), IL-10 (ThermoFisher Scientific, Waltham, MA), and IL-1β (R&D Systems, Minneapolis, MN) were run according to manufacturer's instructions. All samples were run in duplicate and absorbance ratios were read at 450nm.

Immunohistochemistry (IHC): Hairy skin (n=3/condition), glabrous skin (n=3/condition), and DRG (n=3/condition) from WT mice were excised and incubated in 0.06% brefeldin A (BFA) in serum free HBSS for 20 min at room temperature. Half of the samples were incubated in inflammatory soup (IS) (10uM; bradykinin triacetate, histamine dihydrochloride, serotonin hydrochloride, prostaglandin E2 dissolved in normal cerebral spinal fluid, pH 6.0) or serum-free media (Kessler et al., 1992; Hachisuka et al., 2016). Incubation in IS or serum-free media occurred for 24 hours (Kessler et al., 1992). Spinal cords from inflamed or naïve WT mice were isolated 24 hours following CFA treatment or from designated naïve controls. Prior to tissue collection,

mice were intracardially perfused with 0.06% BFA in 0.9% saline for 20 min and then perfused with 4% paraformaldehyde. All samples were post-fixed overnight in 4% paraformaldehyde (PFA), cryoprotected overnight in 30% sucrose, and later embedded in Optimal Cutting Temperature (OCT) prior into 30 μm cross sections using a cryostat. Tissue sections were briefly washed with sterile PBS and incubated with staining buffer (0.05% triton and 30% fetal bovine serum in PBS) solution for 40 min at room temperature. Slices were then incubated with primary unconjugated antibodies for 48 hours at 4°C. The following primary antibodies were diluted in staining buffer: monoclonal anti-mouse cytokeratin 14 (K14; Abcam, Cambridge, United Kingdom; 1:300 dilution), polyclonal anti-goat TIMP-1 (R&D Systems; Minneapolis, MN; 1:300 dilution), monoclonal anti-mouse Microtubule-associated protein 2 (MAP2; Millipore Sigma, Burlington, MA; 1:1000 dilution), and monoclonal anti-mouse primary conjugated-cy3 glial fibrillary acidic protein (GFAP; Abcam, Cambridge, United Kingdom; 1:500 dilution). Secondary antibodies were incubated with tissue slices for 2-3 hours at 4°C. The following secondary antibodies were diluted in staining buffer: polyclonal rabbit anti-mouse Alexa-488 (Life Technologies, Carlsbad, CA, 1:000), polyclonal donkey anti-goat Alexa-568 (Life Technologies, Carlsbad, CA,1:000), and polyclonal goat anti-mouse Alexa-568 (Life Technologies, Carlsbad, CA; 1:1000 dilution). Slides with DRG and spinal cord slices were incubated with 300um DAPI prior to cover-slipping to visualize nuclei of satellite glial cells and astrocytes, respectively.

MMP-9 colorimetric activity: Protein was extracted from the hind paw of wildtype and T1KO mice 1 day post-CFA injections (s.c., 10μL) or from designated naïve controls for a high throughput screening of MMP-9 activity. Gelatinase activity was measured using the SensolyteGeneric MMP colorimetric assay kit (Anaspec, Fremont, CA). Samples were run in duplicate and end-point enzymatic activity was analyzed using a glutathione reference standard.

RT-qPCR: Total RNA from WT and T1KO was extracted from naïve and inflamed samples 1 day post CFA administration using a RNeasy Mini Kit (Qiagen, Venlo, Netherlands). To quantify cutaneous TIMP-2 and TIMP-4 mRNA expression, equal amounts of cDNA were synthesized using the iScript cDNA Synthesis Kit (Bio-Rad Laboratories, Hercules, CA) and mixed with SsoAdvanced Universal SYBR Green Supermix (Bio-Rad Laboratories, Hercules, CA) and 2uM of both forward and reverse primers (see Table 1). GAPDH was amplified as an internal control. The threshold crossing value was noted for each transcript and normalized to the internal control. The relative quantitation of each transcript was performed using the ΔΔCt method and presented as fold change relative to naïve WT expression.

Gene	Forward	Reverse
Timp2	5'- CCAGAAGAAGAGCCTGAACCA-3'	5'- GTCCATCCAGAGGCACTCATC-3'
Timp4	5'- TGCAGAGGGAGAGCCTGAA-3'	5'- GGTACATGGCACTGCATAGCA-3'
Gapdh	5'- ATGAATACGGCTACAGCAACAGG-3'	5'- CTCTTGCTCAGTGTCCTTGCTG-3'

Table 1: Primer sequences for qPCR

Statistical analysis: All data were analyzed using one-way or mixed designs Analysis of Variance (ANOVA). *Post hoc* analyses were performed using Tukey's HSD, and statistical significance was determined using a $p<.05$. Statistical analysis was performed using SPSS (Version 25). Since ANOVAs rely on linear relationships among data, and not all effects can be resolved using linear based statistical tests, we used trend analyses (e.g., contrasts) to test for significant nonlinear relationships in some of our behavioral analyses. An added benefit of this approach is that trend analyses are more robust than ANOVAs (Tabachnick and Fidell, 2007). For the CPP data, clonidine induced CPP was assessed using a 2-way repeated measures ANOVA with post-hoc analysis of pre vs post conditioning time spent in the clonidine paired chamber for each treatment

group using Sidak's multiple comparisons test. Between groups analysis was performed on difference scores calculated as post-conditioning (-) pre-conditioning time spent in the clonidine paired chamber.

RESULTS

Cutaneous TIMP-1 expression is upregulated prior to the onset of inflammatory hypersensitivity

To determine whether cutaneous inflammation alters the expression of TIMP-1 in tissues along the peripheral sensory circuit, we injected emulsified CFA (10 µL, s.c.) into the hairy skin of the ipsilateral hind paw and collected spinal cord (SC; L2-L3), dorsal root ganglia (DRG; L2-L3), and hairy skin over the course of 7 days. We found that inflammation did not alter the overall expression of TIMP-1 protein in SC or DRG, all F's > 1.13, p>.05 (Figure 2 A, B). However, we observed a significant increase in cutaneous TIMP-1 protein 1, 3, 5, and 7 days following CFA administration, $F(4,19) = 37.54$, p<.01 (Figure 2C). To confirm the above results, and to localize the cellular source of TIMP-1 expression, immunohistochemistry (IHC) was performed on DRG and skin samples incubated *in vitro* with or without inflammatory soup (IS)(Kessler et al., 1992), as well as spinal cords following *in vivo* inflammation. Although overall TIMP-1 expression levels were unaltered in the spinal cord and DRG following inflammation, we found that TIMP-1 co-localized with glial fibrillary acidic protein (GFAP) expressing cells following inflammatory stimulation, demonstrating that astrocytes (Figures 2D) and satellite glial cells (Figure 2E) appear to increase levels of TIMP-1 expression following inflammation (Huang et al., 2011; Welser-Alves et al., 2011). We also found that TIMP-1 expression was upregulated in K14-positive keratinocytes in both hairy and glabrous skin following inflammatory stimulation (Figure 2F; glabrous skin data not shown).

To associate the expression of cutaneous TIMP-1 with the development of mechanical hypersensitivity, we assessed paw withdrawal thresholds (PWT) on the plantar surface of the hind paw for 7 days following CFA injection into the dorsal, hairy skin. When we compared the temporal expression of TIMP-1 to the time course of behavioral sensitivity, we found that TIMP-1 protein levels peaked 3 days following CFA administration (see Figure 2C), at a time when mice developed mechanical allodynia, $F(2,12) = 43.94$, $p < 0.05$, Figure 2G. We also assessed TIMP-1 expression in the ventral surface of the hind paw, where we assessed mechanical stimulation and found that CFA-injection into hairy skin caused a concomitant increase in TIMP-1 in glabrous K14-positive keratinocytes (data not shown). Together, these data indicate that cutaneous inflammation induces the expression of TIMP-1 in keratinocytes at the time of inflammation and prior to the onset of mechanical allodynia.

Mice lacking TIMP-1 exhibit hyperalgesia in inflamed and uninflamed cutaneous tissues

To determine whether endogenous TIMP-1 expression is important for the normal progression of hypersensitivity, we used a global TIMP-1 knockout (T1KO) mouse strain. We first assessed behavioral responsiveness to radiant heat on the plantar surface of the hind paw following s.c. administration of a diluted CFA solution. We chose to use a diluted CFA solution because our preliminary experiments suggested that exposure to slight challenges significantly alters sensitivity in T1KO mice (see Figure 1). To ensure that any potential differences in responding to inflammatory stimulation were not due to preexisting differences in sensory thresholds between strains, we measured baseline responding to radiant heat and found no significant differences in paw withdrawal latencies (PWL), $F(1, 31) = .47$, $p > .05$ (Figure 3A). Our analysis failed to detect any significant differences in responding between naïve and WT mice administered diluted (e.g., subthreshold) CFA (Figure 3A). Interestingly, analysis did show that inflamed T1KO mice

exhibited prolonged thermal hyperalgesia following s.c. injection of diluted CFA that persisted for 29 days, all Fs < 2.30, $p < .05$ (Figure 3B).

Next, we assessed mechanical response thresholds (von Frey) following diluted CFA administration. Analysis of baseline responses to mechanical stimulation did not reveal any significant differences between genotypes $F(1, 36) = .34$, $p < .05$ (Figure 3C). We did find that CFA administration reduced mechanical response thresholds in both genotypes $F(1, 34) = 17.61$, $p < .01$. However, T1KO mice exhibited greater mechanical hypersensitivity 1 day following CFA treatment, compared to WT controls, all Fs < 4.59, p <.05 (Figure 3D). Thus, we concluded that the presence of TIMP-1 delays the onset of hypersensitivity, and that the absence of TIMP-1 results in a rapidly developing hypersensitivity.

To determine whether the rapid emergence of inflammatory hypersensitivity in T1KO mice was due to compensatory expression of *Timp2* or *Timp4* mRNA, we examined cutaneous expression of each transcript in naïve and inflamed T1KO mice. We found no significant differences in the basal expression of either transcript in WT or T1KO mice. However, *Timp2* and *Timp4* expression decreased in T1KO mice following inflammation (Figure 4A, B), suggesting that genetic deletion of TIMP-1 does not result in a compensatory response from other TIMPs, all *Fs* < 11.65, $p < 0.01$.

Our current data demonstrate that cutaneous TIMP-1 is an early emergent protein following inflammation, and that in the absence of TIMP-1 the development of hypersensitivity is accelerated. Therefore, TIMP-1 signaling may also have important implications for regulating the development of inflammatory hypersensitivity in tissue adjacent to the site of inflammation that is innervated by afferent terminals that are different from those that innervate inflamed skin. To test this possibility, we assessed the development of hypersensitivity in the glabrous skin following

injection of diluted CFA into hairy skin in both T1KO and WT following baseline assessment of sensitivity. Again, we observed no genotype-specific differences in baseline reactivity, and because of this consistent finding, we will no longer present data depicting baseline behavioral reactivity. Analysis using an ANOVA revealed that T1KO mice, relative to WT mice, exhibited increased sensitivity to mechanical stimulation on the plantar surface of the hindpaw following inflammation of hairy skin that was not temporally dependent, all Fs < 4.41, p <.05, (Figure 5A, B). Additional analysis using trend analyses, however, revealed that inflamed T1KO mice exhibited increased inflammatory hypersensitivity 1 day following CFA treatment when compared to all other mice, $F(1,57) = 11.55$, p <.01 (Figure 5A).

To examine whether inflammatory hypersensitivity on the plantar surface of the hindpaw could be prevented by administration of rmTIMP-1, and the potential signaling mechanism by which the effect of rmTIMP-1 alleviates hypersensitivity, T1KO mice received injections of 3 different recombinant constructs of the TIMP-1 protein, full-length rmTIMP-1 [TIMP-1(FL)], the truncated N terminus peptide [TIMP-1(N)] that retains MMP inhibitory function but no cell signaling capacity, or the truncated C terminus peptide [TIMP-1(C)]) that lacks MMP inhibitory capacity but retains its cell signaling function at the time of CFA administration. To limit the complexity of our experimental design, and to determine the optimal dose for the administration of each TIMP-1 construct, we conducted a pilot experiment using a small cohort of T1KO mice given 1, 10, or 100 ng/µL of TIMP-1 at the time of inflammation. We found that 10 ng/µL was effective at reducing inflammatory hypersensitivity (data not shown). We then administered a separate cohort of T1KO mice 10 ng/µL of TIMP-1(FL), TIMP-1(N), or TIMP-1(C) at the time of CFA administration. Mechanical hypersensitivity was assessed 24 hours later. While inflamed T1KO mice exhibited a significant reduction in mechanical thresholds, T1KO mice treated with

the TIMP-1 constructs did not. Moreover, we observed no significant differences in the response thresholds between mice given TIMP-1(FL), TIMP-1(N), or TIMP-1(C), all Fs > 4.54, p < .01 (Figure 5C), demonstrating that MMP-dependent and MMP-independent signaling mechanisms contribute to the attenuation of inflammatory hypersensitivity by TIMP-1.

The above data show that inflammation in one somatic region could lead to mechanical hypersensitivity in tissue distal to the site of inflammation, reminiscent of "mirror image pain" (Treede et al., 1992; Treede et al., 2015). To test this possibility, we inflamed one hindpaw and measured mechanical sensitivity on the opposite hindpaw for 7 days following CFA administration. We also examined whether treatment with rmTIMP-1 at the site and time of inflammation affected sensitivity. We found that inflamed T1KO mice exhibited contralateral mechanical hypersensitivity over the course of 7 days following CFA-injection relative to WT mice (Figure 5D). Interestingly, this contralateral hypersensitivity was prevented by treatment with rmTIMP-1 in T1KO mice, F (4, 43) = 5.52, $p < 0.05$ (Figure 5D).

The lack of TIMP-1 does not alter the expression of local inflammatory molecules

TIMP-1 is primarily known as a broad-spectrum MMP inhibitor, and because MMPs are known to contribute to hypersensitivity, we hypothesized that the absence of TIMP-1 may cause hypersensitivity due to elevated activity and expression of MMP-9 (Kawasaki et al., 2008; Brew and Nagase, 2010). Examination of hairy skin collected 1 day following CFA from WT and T1KO mice demonstrated that there was an inflammation-induced increase in both MMP-9 expression and activity, all Fs > 7.61, p <.05 but that these effects were not genotype-specific, all Fs < 2.05, p >.05 (Figure 6A, B). The TIMP/MMP axis also regulates the proteolytic maturation of inflammatory molecules which can cause hypersensitivity (Pagenstecher et al., 1998; Ellis and Bennett, 2013). We next assessed whether the absence of TIMP-1 during inflammation caused

elevated expression in skin. Using ELISAs, we assessed the expression of cutaneous IL-1β, IL-6, TNF-α, and IL-10 at 1 day following CFA-injection. Analysis revealed an inflammation-induced increase in IL-1β and IL-6 expression (Figure 6C, D) all Fs > 12.94, p <.05. In comparison, analysis of TNF-α and IL-10 did not reveal any significant differences following inflammation or between genotypes, all Fs < 4.64, p > .05 (Figure 6E, F). These data suggest that TIMP-1 does not affect the normal progression of hypersensitivity through the known MMP regulatory or cytokine-dependent mechanisms.

Administration of recombinant TIMP-1 attenuates ongoing pain in WT mice.

Previous experiments demonstrate that the administration of rmTIMP-1 attenuates evoked mechanical and thermal hypersensitivity in T1KO mice. Here, we examined whether the administration of rmTIMP-1 also attenuated ongoing pain in WT mice using CPP (as described in Methods; (King et al., 2009); Figure 7A). Analysis of pre- compared to post-conditioning time spent in the chamber indicate an effect of drug (F (1, 30) = 7.269, p<0.05), with post-hoc analysis confirming an increase in post-conditioning time spent in the clonidine paired chamber compared to pre-conditioning time in vehicle treated mice (p<0.01) but not in rmTIMP-1 treated mice (p>0.05) (Figure 7B). These observations indicate that mice administered CFA and TIMP-1 did not demonstrate clonidine-induced CPP (Figure 7B, C). Because clonidine is only effective when pain is present (King et al., 2009), these results suggest that treatment with rmTIMP-1 attenuated ongoing inflammatory pain.

DISCUSSION

Although TIMP-1 is known to regulate ECM dynamics, inflammation, and wound healing, previous reports suggest that TIMP-1 may also play a role in the emergence of pain, particularly following nerve damage (Kawasaki et al., 2008; Ji et al., 2009; Huang et al., 2011). However, the

protective function of TIMP-1 in the development of inflammatory hypersensitivity required further investigation. Previous RNA sequencing results shows that TIMP-1 mRNA is present throughout the CNS and peripheral nervous systems (PNS) (Fagerberg et al., 2010). In the adult mouse model, TIMP-1 expression is low during basal conditions but can be induced following insult to nervous system (Crocker et al., 2006; Parkitna et al., 2006; McKelvey et al., 2015). Therefore, we first determined that cutaneous inflammation alters TIMP-1 expression proximal to the location of inflammation as well as distal locations associated with increased hypersensitivity. Furthermore, cutaneous inflammation induced TIMP-1 protein levels within 24 hr, peaked at 3 days, and waned by day 7. These data compliment other studies that suggest that TIMP-1 is inducible, immediate factor involved in the rapid response to tissue damage(Crocker et al., 2006; Kawasaki et al., 2008).

TIMP-1 is expressed by a variety of cell types including astrocytes and oligodendrocytes, endothelial cells, fibroblasts, mast cells, and keratinocytes (Yokose et al., 2012; Claycomb et al., 2013). Using an *in vitro* model of inflammation, we determined that cutaneous TIMP-1 expression was induced in K14-positive keratinocytes within 24 hr. These results agree with prior work showing keratinocytes upregulate TIMP-1 following UVB photodamage (Yokose et al., 2012). Furthermore, given that keratinocytes augment nociceptive signaling through the release of neuroactive molecules, TIMP-1 may be released from keratocytes to attenuate nociceptive responsiveness immediately following tissue damage (Fagerberg et al., 2010; Yokose et al., 2012; Baumbauer et al., 2015; Edqvist et al., 2015; Moehring et al., 2018). However, the effect of TIMP-1 may depend on the type of insult experienced. A recently published gene array comparing gene expression profiles in rats following chronic constriction injury (CCI) of the sciatic nerve or s.c. administration of CFA, and found that TIMP-1 mRNA was increased within 3 days following

nerve damage in the spinal cord and DRG but not following cutaneous inflammation (Parkitna et al., 2006). While we also reported no changes in overall TIMP-1 protein expression in the spinal cord or DRG following inflammation, we did observe increased TIMP-1 expression in GFAP expressing cells in both structures, suggesting that inflammation increases TIMP-1 expression in astrocytes and satellite glial cells (SGCs), respectively. Interestingly, previous work has shown that peripheral nerve injury increases TIMP-1 in SGCs (Parkitna et al., 2006; Huang et al., 2011), and that experimental autoimmune encephalomyelitis increases TIMP-1 in astrocytes (Pagenstecher et al., 1998; Claycomb et al., 2013).

To test whether local TIMP-1 expression is important for regulating the onset of inflammatory hypersensitivity, we used global TIMP-1 knockout mouse and assessed thermal and mechanical responding in response to inflammation. We found that inflamed T1KO mice developed exaggerated nocifensive responses to mechanical and thermal stimulation at the site of inflammation that was not observed in WT mice. This is important because it demonstrates that in the absence of TIMP-1, subtle perturbations can result in profound functional changes in sensory processing. Indeed, we observed such an effect when T1KO mice were administered s.c. injections of physiological saline. Our results further suggest that TIMP-1 may have an active role in regulating responding to injury and inflammation, specifically, and sensory stimulation, in general.

To determine whether T1KO mice develop a pathological pain-like phenotype following inflammation, we assessed mechanical thresholds in tissue adjacent (innervated by different sets of afferents) and contralateral to inflammation. We found that mice lacking TIMP-1 exhibited mechanical sensitivity in both adjacent and distal skin This gain of sensitivity in uninjured tissues is often specific to mechanical stimulation and is associated with the development of pathological pain (Treede et al., 1992; Treede et al., 2015), suggesting that TIMP-1 may have a yet to be defined

role in the regulation of normal somatosensation. In further support of this conclusion, hypersensitivity in both the tissue adjacent and distal to inflammation was attenuated when rmTIMP-1 was administered to T1KO mice at the site of inflammation. These data suggest that inflammation induces TIMP-1 expression in a coordinated fashion that influences the normal progression of inflammatory sensitivity. Consequently, as is the case for T1KO mice, dysfunction in TIMP-1 signaling, may lead to an aberrant process that encourages the transition from acute to chronic pain.

Because TIMP-1 is primarily characterized as an inhibitor of MMP activity, and MMPs have a known role in driving pain following nerve injury (Kawasaki et al., 2008; Remacle et al., 2018). We hypothesized that disrupting the TIMP/MMP balance would cause increased hypersensitivity through MMP and proinflammatory cytokine signaling. However, we failed to observe any genotype-specific differences in the expression of MMP-9 or cytokines in the skin following inflammation. This suggested to us that TIMP-1 may be inhibiting development of hypersensitivity by a receptor-mediated mechanism. Supporting this, administration of the truncated C-terminal of TIMP-1 that retains cell signaling function ameliorates inflammatory hypersensitivity. However, given that the truncated MMP-inhibitory N-terminal domain also attenuated hypersensitivity, we cannot rule out the role of MMP-inhibition in the regulation of pain, nor do we posit that the effects of TIMP-1 are solely due to a cell signaling event. What we do propose is that TIMP-1 may act through both pathways to effectively attenuate pain progression. This latter point may help to explain, at least in part, why small molecule inhibitors of MMP activity have limited efficacy. By targeting the entire TIMP-1 pathway, we may be able to effectively manage pain progression. Moreover, the site of TIMP-1 administration may also determine efficacy. TIMPs and MMPs are ubiquitously expressed throughout all tissues, and may

have divergent responses to changing physiological environments. If administration of TIMP-1 occurs directly at the site of injury (or sensitivity), efficacy may be increased by precisely targeting the tissue affected by pain or injury, while simultaneously avoiding disrupting the TIMP/MMP balance in unaffected tissue.

Finally, demonstrating that TIMP-1 alleviates ongoing pain in WT mice, in conjunction with our previously described data, identifies TIMP-1 as a potential clinical target. One lingering concern was that administration of rmTIMP-1 may result in levels cutaneous TIMP-1 that were beyond normal physiological levels. However, it should be noted that this is a common occurrence when drugs are used to treat clinical conditions, including pain, and targeting TIMP-1 may a novel molecule for the development of therapeutics for pain management.

Figure 1.

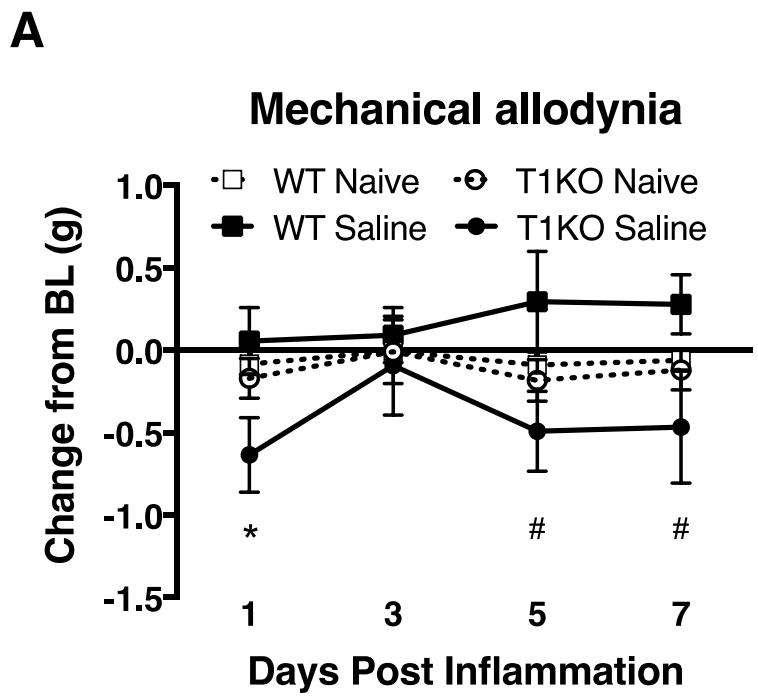
A
Mechanical allodynia
WT Naive
T1KO Naive
WT Saline
T1KO Saline
Change from BL (g)
1.0
0.5
0.0
-0.5
-1.0
-1.5
*
#
#
1
3
5
7
Days Post Inflammation

Figure 2.

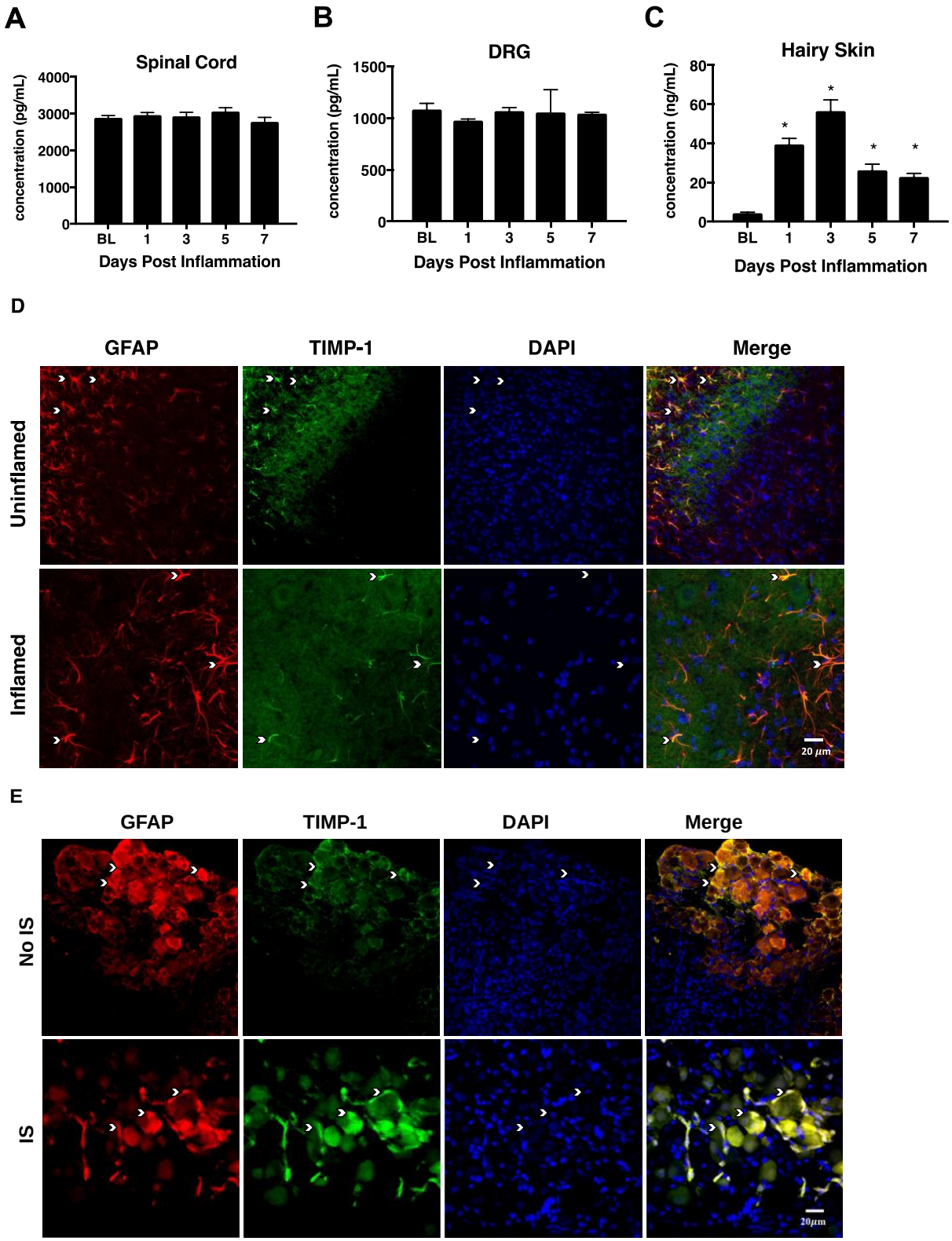
A
Spinal Cord
concentration (pg/mL)
4000
3000
2000
1000
0
BL
1
3
5
7
Days Post Inflammation
B
DRG
concentration (pg/mL)
1500
1000
500
0
BL
1
3
5
7
Days Post Inflammation
C
Hairy Skin
concentration (ng/mL)
80
60
40
20
0
BL
1
3
5
7
Days Post Inflammation
D
GFAP
TIMP-1
DAPI
Merge
Uninflamed
Inflamed
20 μm
E
GFAP
TIMP-1
DAPI
Merge
No IS
IS
20μm

F

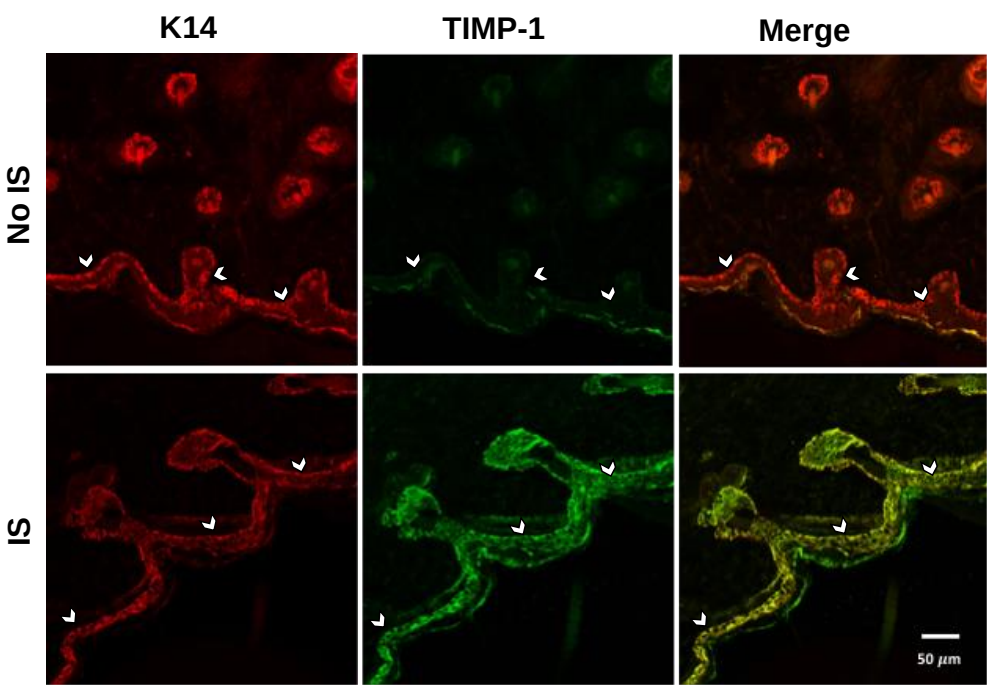
K14
TIMP-1
Merge
No IS
IS
50 μm

G

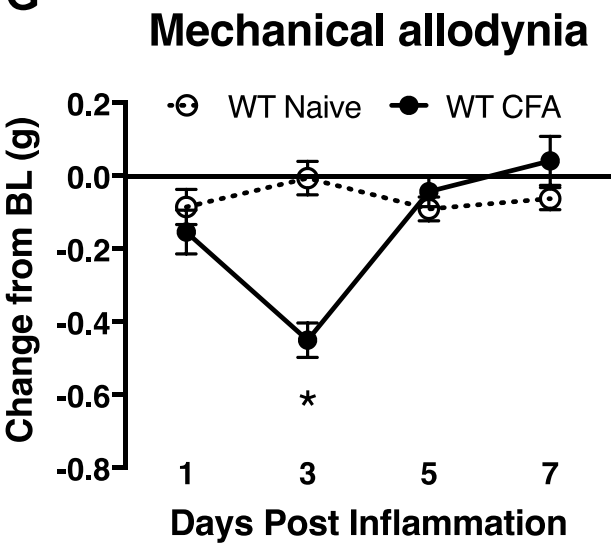
Mechanical allodynia
WT Naive
WT CFA
Change from BL (g)
0.2
0.0
-0.2
-0.4
-0.6
-0.8
*
1
3
5
7
Days Post Inflammation

Figure 3

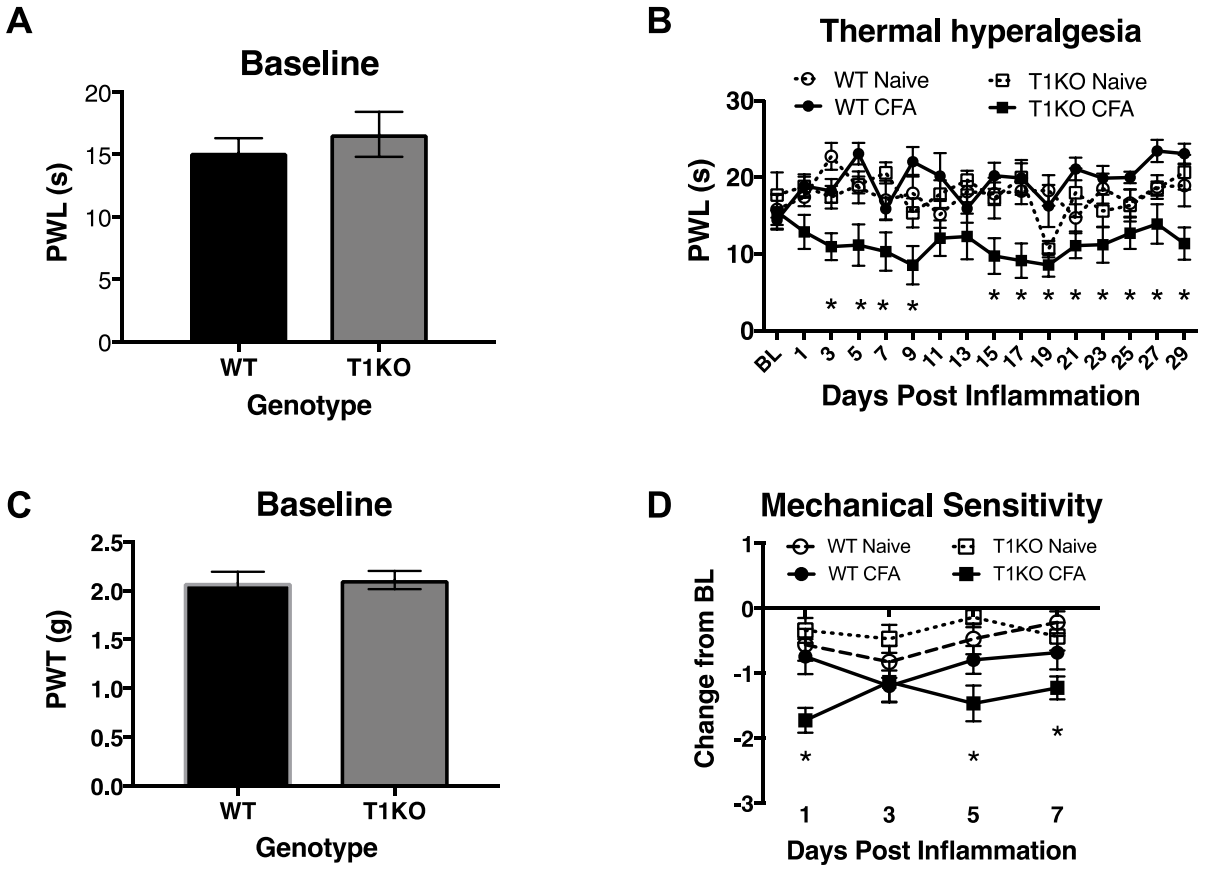
A
Baseline
PWL (s)
20
15
10
5
0
WT
T1KO
Genotype
B
Thermal hyperalgesia
WT Naive
WT CFA
T1KO Naive
T1KO CFA
PWL (s)
30
20
10
0
BL 1 3 5 7 9 11 13 15 17 19 21 23 25 27 29
Days Post Inflammation
C
Baseline
PWT (g)
2.5
2.0
1.5
1.0
0.5
0.0
WT
T1KO
Genotype
D
Mechanical Sensitivity
WT Naive
WT CFA
T1KO Naive
T1KO CFA
Change from BL
1
0
-1
-2
-3
1 3 5 7
Days Post Inflammation

Figure 4

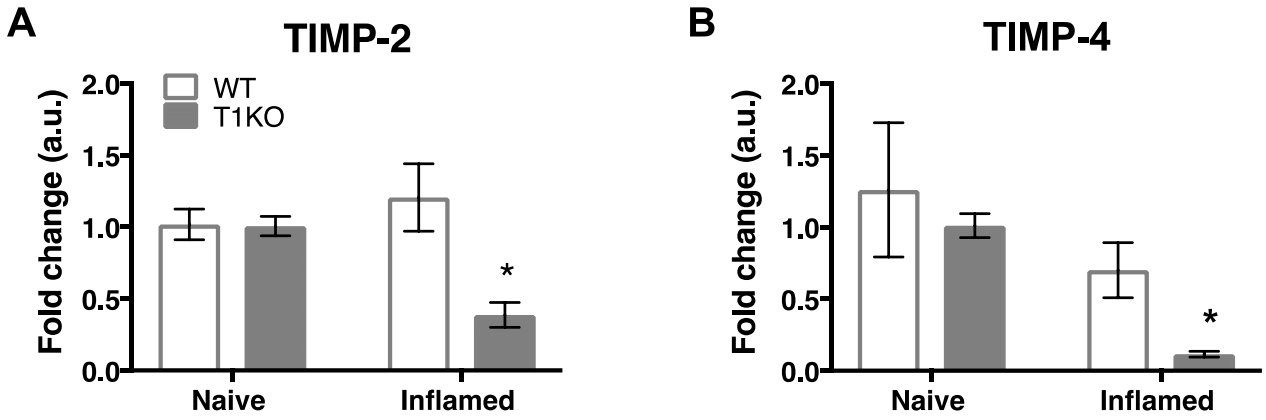
A
TIMP-2
WT
T1KO
Fold change (a.u.)
2.0
1.5
1.0
0.5
0.0
*
Naive
Inflamed
B
TIMP-4
Fold change (a.u.)
2.0
1.5
1.0
0.5
0.0
*
Naive
Inflamed

Figure 5

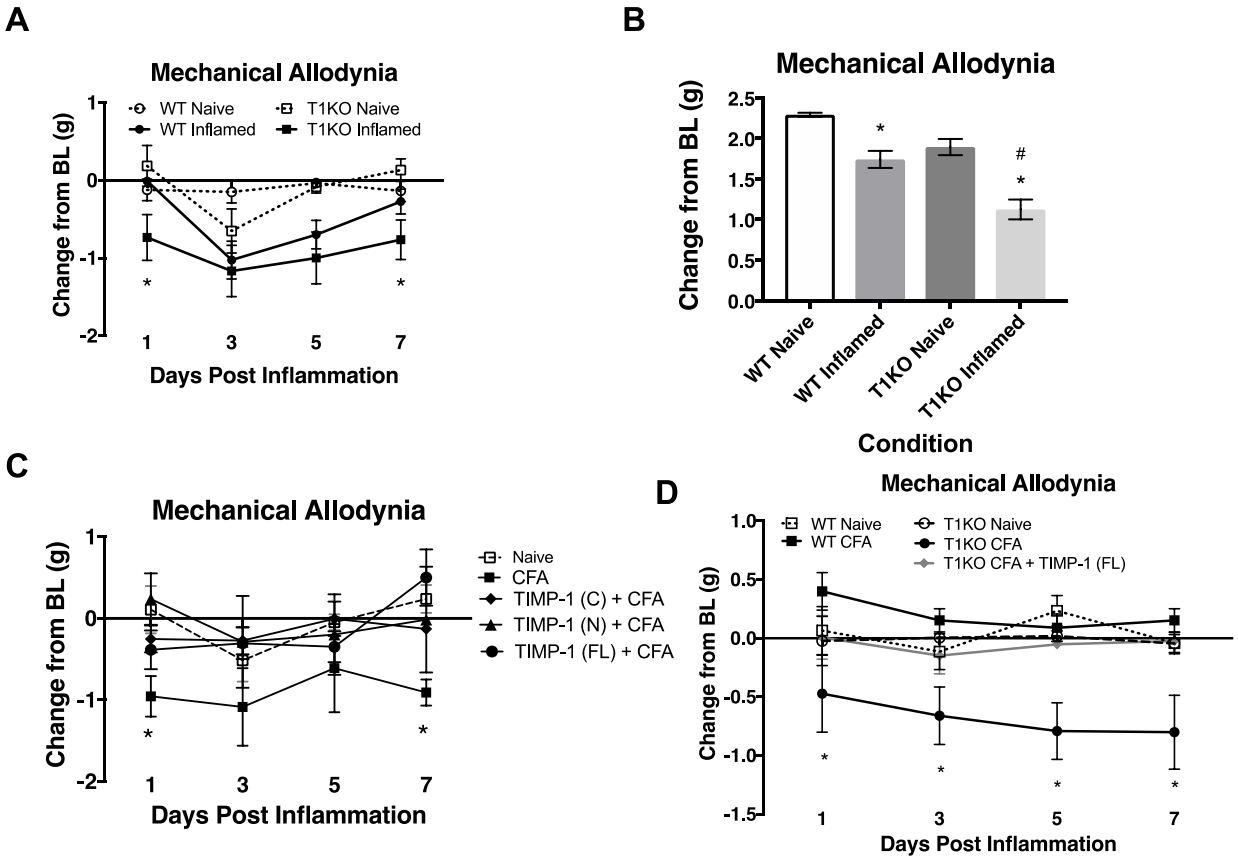
A
Mechanical Allodynia
WT Naive
WT Inflamed
T1KO Naive
T1KO Inflamed
Change from BL (g)
Days Post Inflammation
B
Mechanical Allodynia
Change from BL (g)
WT Naive
WT Inflamed
T1KO Naive
T1KO Inflamed
Condition
C
Mechanical Allodynia
Naive
CFA
TIMP-1 (C) + CFA
TIMP-1 (N) + CFA
TIMP-1 (FL) + CFA
Change from BL (g)
Days Post Inflammation
D
Mechanical Allodynia
WT Naive
WT CFA
T1KO Naive
T1KO CFA
T1KO CFA + TIMP-1 (FL)
Change from BL (g)
Days Post Inflammation

Figure 6.

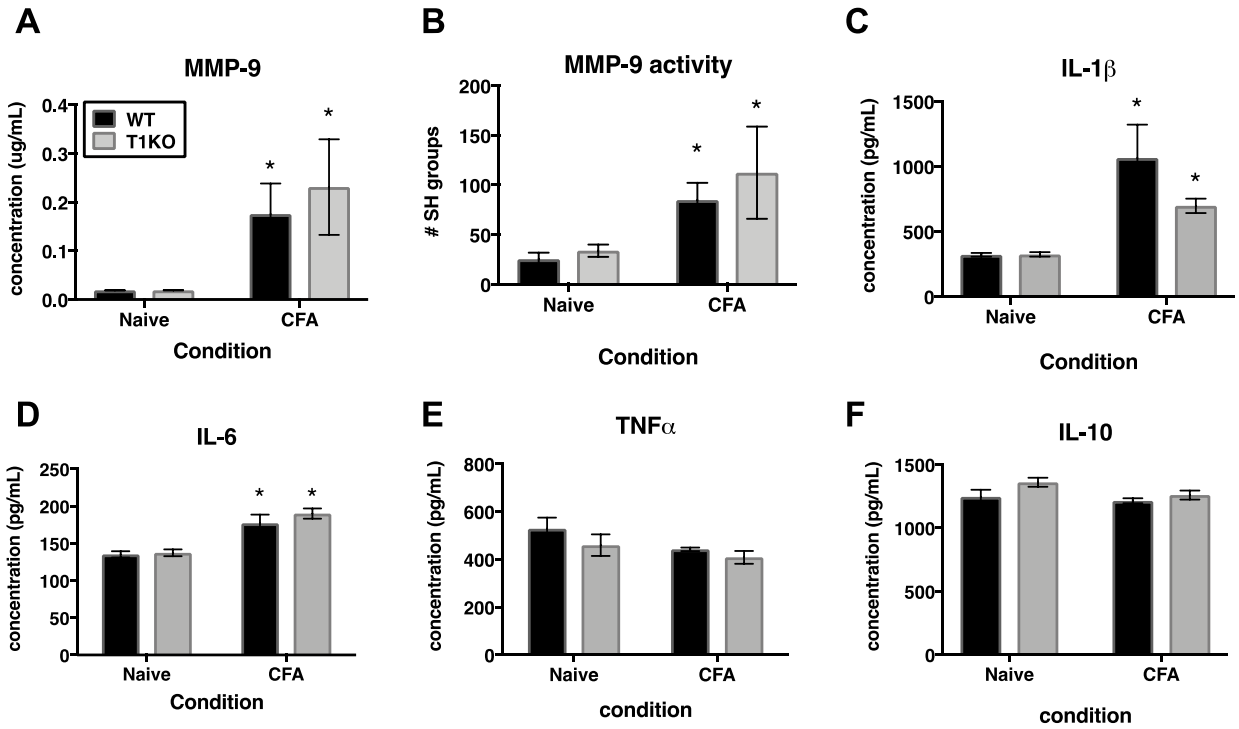
A
MMP-9
WT
T1KO
concentration (ug/mL)
0.4
0.3
0.2
0.1
0.0
Naive
CFA
Condition
B
MMP-9 activity
SH groups
200
150
100
50
0
Naive
CFA
Condition
C
IL-1β
concentration (pg/mL)
1500
1000
500
0
Naive
CFA
Condition
D
IL-6
concentration (pg/mL)
250
200
150
100
50
0
Naive
CFA
Condition
E
TNFα
concentration (pg/mL)
800
600
400
200
0
Naive
CFA
condition
F
IL-10
concentration (pg/mL)
1500
1000
500
0
Naive
CFA
condition

Figure 7.

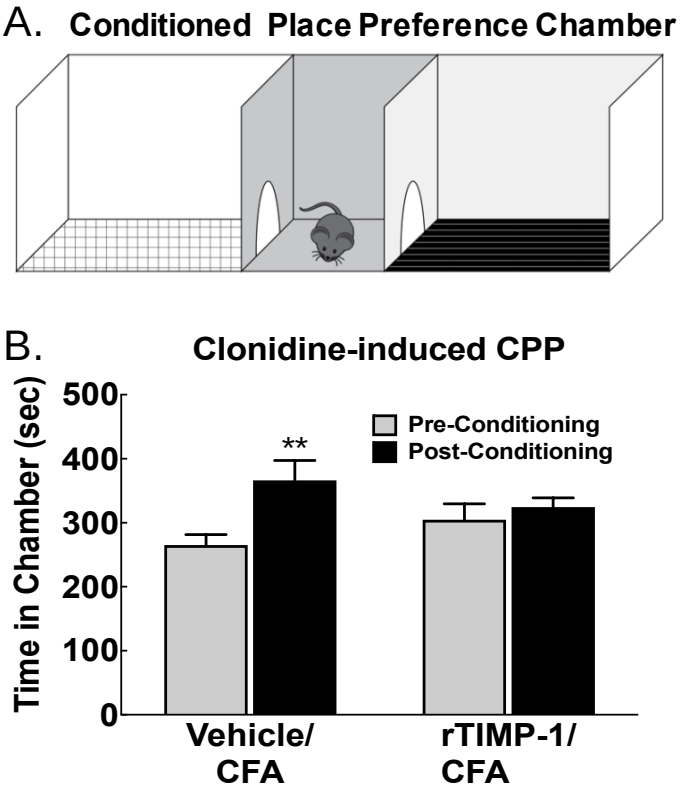
A. Conditioned Place Preference Chamber
B. Clonidine-induced CPP
Time in Chamber (sec)
500
400
300
200
100
0
**
Pre-Conditioning
Post-Conditioning
Vehicle/ CFA
rTIMP-1/ CFA

Figure 1. **Saline injection causes hypersensitivity in mice lacking TIMP-1**.

Paw withdrawal thresholds (PWT) presented as change from baseline in grams following s.c. injection of 0.9% saline. T1KO mice administered saline exhibited a significant reduction in mechanical thresholds 1 day following injection compared to WT controls (n=6/condition). * indicate significant differences compared to naïve controls, $p<.05$, and error bars depict SEM.

Figure 2. **Assessing TIMP-1 expression along peripheral nociceptive circuit following cutaneous inflammation**.

(A) Cutaneous inflammation does not alter overall TIMP-1 protein expression in lumbar spinal cord or (B) DRG, but does increase protein expression in (C) hairy skin. n=4/condition (D) Immunostaining (20X) of naïve and inflamed lumbar spinal cord 24 hr following inflammation. TIMP-1 (green) expression is localized to GFAP-positive astrocytes (red). n=3/condition, scale bar 20 μm. (E) Immunostaining (20X) of naïve and inflamed lumbar DRG 24 hr following inflammation. TIMP-1 (green) expression is colocalized with by GFAP-positive satellite glial cells (red). n=3/condition, scale bar 20 μm. (F) Immunostaining (40X) of hind paw hairy skin shows K14-positive keratinocytes (red) upregulate TIMP-1 (green) 24hrs following inflammation compared to naïve control. n=3/condition, scale bar 50 μm. (G) Assessment of mechanical hypersensitivity over 7 days following s.c. administration of CFA. Inflamed mice show a significant reduction in mechanical thresholds relative to naïve mice 3 days following inflammation (n=6/condition). * indicate significant differences compared to naïve controls, $p<.05$, and error bars depict SEM.

Figure 3: **Mice lacking TIMP-1 develop thermal and mechanical hypersensitivity following cutaneous inflammation**.

(A) No differences in baseline thermal PWL are exhibited between T1KO and WT mice (n=16/condition). (B) Inflamed T1KO mice exhibit significantly reduced PWLs compared to inflamed WT mice and naïve WT and T1KO mice (n=8/condition). (C) Baseline assessment of mechanical PWTs revealed no genotypic differences between T1KO (n=20) and WT mice (n=18). (D) T1KO mice develop significantly reduced PWTs 1 day following CFA administration compared to WT controls (n=8-10/condition).

Figure 4: Assessment of cutaneous TIMP-2 and TIMP-4 mRNA expression following inflammation

(A) TIMP-2 mRNA expression is decreased in T1KO mouse skin 1 day following inflammation relative to WT controls. (B) TIMP-4 mRNA expression is decreased 1 day following CFA compared to WT inflamed mice. n=4/condition, * indicate significant differences compared to naïve controls, $p<.05$, and error bars depict SEM.

Figure 5: Mice lacking TIMP-1 show increased sensitivity in non-inflamed tissues

(A) Injection of CFA into the hairy skin causes mechanical hypersensitivity on the plantar surface of the paw to develop 1 day following inflammation in T1KO, but not WT, mice. (B) Graph depicting mechanical responsiveness following inflammation collapsed across time. Inflamed T1KO mice are more mechanically sensitive overall following cutaneous inflammation. (C) Administration of TIMP-1(FL), TIMP-1(N), or TIMP-1(C) into the hairy skin at the time of inflammation prevents the development of mechanical hypersensitivity in T1KO mice. (D) Hindpaw administration of CFA produces mechanical hypersensitivity on the paw contralateral to inflammation in T1KO relative to WT mice. Treatment with rmTIMP-1 attenuated contralateral hypersensitivity in T1KO mice. PWT are presented as change from baseline. n=8/condition, * represent significant differences relative to naïve controls, $p<.05$, and error bars depict SEM.

Figure 6. Inflammation does not alter pro-inflammatory molecules in a genotype-specific manner.

A) Cutaneous inflammation significantly increases MMP-9 protein expression in WT and T1KO skin 1 day following CFA administration (n=7/condition). B) Cutaneous inflammation increases MMP-9 activity in WT and T1KO hairy skin 1 day following CFA administration. C) Cutaneous inflammation significantly increases IL-1β protein expression in WT and T1KO hairy skin 1 day following inflammation. D) Cutaneous inflammation significantly increases IL-6 protein expression in WT and T1KO hairy skin 1 day following CFA administration. E) Cutaneous inflammation does not affect expression of TNF-α following CFA administration. F) Cutaneous inflammation does not affect expression of IL-10 protein in WT and T1KO skin following CFA administration. n=4/condition, * represent significant differences relative to naïve controls, $p<.05$, and error bars depict SEM.

Figure 7. Replacement of TIMP-1 attenuates ongoing inflammatory pain in WT mice.

A) Schematic of 3-chamber CPP box. B). Comparison of pre-conditioning and post-conditioning time spent in the clonidine paired chamber show a significant increase in the post-conditioning time in the Vehicle/CFA treated mice, but not the rTIMP-1/CFA treated mice. **$p<0.01$ vs pre-conditioning time. Sample size CFA/rTIMP-1 = 9; CFA/Veh = 8. Error bars = S.E.M.

REFERENCES

Allchorne, A., Broom, D., and Woolf, C. (2005). Detection of cold pain, cold allodynia and cold hyperalgesia in freely behaving rats. *Molecular Pain* 1(36)**,** 1-9.

Baker, A., Edwards, D., and Murphy, G. (2002). Metalloproteinase inhibitors: biological actions and therapeutic opportunities. *Journal of Cell Science* 1115**,** 3719-3727.

Baumbauer, K.M., DeBerry, J.J., Adelman, P.C., Miller, R.H., Hachisuka, J., Lee, K.H., et al. (2015). Keratinocytes can modulate and directly initiate nociceptive responses. *eLife*.

Brew, K., and Nagase, H. (2010). The tissue inhibitors of metalloproteinases (TIMPs): An ancient family with structural and functional diversity. *Biochim Biophys Acta*.

Cathcart, J., and Cao, J. (2015). MMP Inhibitors: Past, present and future. *Frontiers in Bioscience* 20.

Claycomb, K., Johnson, K., Winokur, P., Sacino, A., and Crocker, S. (2013). Astrocyte regulation of CNS inflammation and remyelination. *Brain Sci* 3(3)**,** 1109-1127. doi: 10.3390/brainsci3031109.

Crocker, S., Whitmire, J., Frausto, R., Chertboonmuang, P., Soloway, P., Whitton, J., et al. (2006). Persistent macrophage/microglial activation and myelin disruption after experimental autoimmune encephalomyelitis in tissue inhibitor of metalloproteinase-1-deficient mice. *The American Journal of Pathology* 169(6).

Dixon, W. (1980). Efficient analysis of experimental observations. *Ann. Rev. Pharmacol. Toxicolology* 20.

Edqvist, P.H.D., Fagerberg, L., Hallström, B.M., Danielsson, A., Edlund, K., M., U.n., et al. (2015). Expression of human skin-specific genes defined by transcriptomics and antibody-based profiling.

Ellis, A., and Bennett, D. (2013). Neuroinflammation and the generation of neuropathic pain. *British Journal of Anaesthesia* 111(1).

Fagerberg, L., Jonasson, K., von Heijne, G., Uhlen, M., and Berglund, L. (2010). Prediction of the human membrane proteome. *Proteomics* 10.

Gardner, J., and Ghorpade, A. (2003). Tissue Inhibitor of Metalloproteinase (TIMP)-1: The TIMPed Balance of Matrix Metalloproteinases in the Central Nervous System. *Journal of Neuroscience Research* 74(6).

Hachisuka, J., Baumbauer, K., Omori, Y., Snyder, L., Koerber, H., and Ross, S. (2016). Semi-intact ex vivo approach to investigate spinal somatosensory circuits. *eLIFE* 5.

Hargreaves, K., Dubner, R., Brown, F., Flores, C., and Joris, J. (1988). A new and sensitive method for measuring thermal nociception in cutaneous hyperalgesia. *Pain* 32(1)**,** 77-88.

Huang, B., Zhao, X., Zheng, L., Zhang, L., Ni, B., and Wang, Y. (2011). Different expression of tissue inhibitor of metalloproteinase family members in rat dorsal root ganglia and their changes after peripheral nerve injury. *Neuroscience* 193**,** 421-428. doi: 10.1016/j.neuroscience.2011.07.031.

Imbe, H., and Kimura, A. (2017). Attenuation of pCREB and Egr1 expression in the insular and anteriorcingulate cortices associated with enhancement of CFA-evoked mechanicalhypersensitivity after repeated forced swim stress. *Brain Research Bulletin* 134(2017)**,** 253-261.

Jankowski, M., Rau, K., Soneji, D., Ekmann, K., Anderson, C., Molliver, D., et al. (2012). Purinergic receptor P2Y1 regulates polymodal C-fiber thermal thresholds and sensory neuron phenotypic switching during peripheral inflammation. *Pain* 153(2)**,** 410-419.

Ji, R., Xu, Z., Wang, X., and Lo, E. (2009). MMP regulation of neuropathic pain. *Trends Pharmacol Sci* 30(7).

Jourquin, J., Tremblay, E., Bernard, A., Charton, G., Chaillan, F.A., Marchetti, E., et al. (2005). Tissue inhibitor of metalloproteinases-1 (TIMP-1) modulates neuronal death, axonal plasticity, and learning and memory. *European Journal of Neuroscience* 22**,** 9.

Kawasaki, Y., Xu, Z., Wang, X., Park, J., Zhuang, Z., Tan, P., et al. (2008). Distinct roles of matrix metalloproteases in the early- and late-phase development of neuropathic pain. *Nature Medicine* 14(3)**,** 5.

Kehlet, H., Jensen, T.S., and Woolf, C.J. (2006). Persistent postsurgical pain: risk factors and prevention. *Lancet* 367(9522)**,** 1618-1625. doi: 10.1016/S0140-6736(06)68700-X.

Kessler, W., Kirchhoff, C., Reeh, P., and Handwerker, H. (1992). Excitation of cutaneous afferent nerve endings in vitro by a combination of inflammatory mediators and conditioning effect of substance P. *Experimental Brain Research* 91(3)**,** 467-476.

Kim, Y., Remacle, A., Chernov, A., Liu, H., Shubayev, I., Lai, C., et al. (2012). The MMP-9/TIMP-1 Axis Controls the Status of Differentiation and Function of Myelin-Forming Schwann Cells in Nerve Regeneration. *PLoS ONE* 7(3).

King, T., Vera-Portocarrero, L., Gutierrez, T., Vanderah, T., Dussor, G., Lai, J., et al. (2009). Unmasking the tonic-aversive state in neuropathic pain. *Nature Neuroscience* 12(11)**,** 1364-1366.

Kouwenhoven, M., Ozenci, V., Gomes, A., Yarilin, D., Giedraitis, V., Press, R., et al. (2001). Multiple sclerosis: elevated expression of matrix metalloproteinases in blood monocytes. *Journal of Autoimmunity* 16(4)**,** 463-470.

Lee, M., Yoon, B., Osiewicz, K., Preston, M., Bundy, B., van Heeckeren, A., et al. (2005). Tissue inhibitor of metalloproteinase 1 regulates resistance to infection. *Infection and Immunity* 73(1)**,** 4.

Li, Y., Lu, Y., Zhao, Z., Wang, J., Li, J., Wang, W., et al. (2016). Relationships of MMP-9 and TIMP-1 proteins with chronic obstructive pulmonary disease risk: A systematic review and meta-analysis. *Journal of Research in Medical Sciences* 21(12).

Martinho, F., Teixeira, F., Cardoso, F., Ferreira, N., Nascimento, G., Carvalho, C., et al. (2016). Clinical investigation of matrix metalloproteinases, tissue inhibitors of matrix metalloproteinases, and matrix metalloproteinase/tissue inhibitors of matrix metalloproteinase complexes and their networks in apical periodontitis. *Basic Research Biology* 42(7).

McKelvey, R., Berta, T., Old, E., Ji, R., and Fitzgerald, M. (2015). Neuropathic pain is constitutively suppressed in early life by anti-inflammatory neuroimmune regulation. *Neurobiology of Disease* 35(2)**,** 457-466.

Moehring, F., Cowie, A., Menzel, A., Weyer, A., Grzybowski, M., Arzua, T., et al. (2018). Keratinocytes mediate innocuous and noxious touch via ATP-P2X4 signaling. *eLife* 7.

Moore, C., and Crocker, S. (2012). An Alternate Perspective on the Roles of TIMPs and MMPs in Pathology. *The American Journal of Pathology*.

Nagase, H., Meng, Q., Malinovskii, V., Huang, W., Chung, L., Bode, W., et al. (1999). Engineering of selective TIMPs. *Annals of the New York Academy of Sciences* 878(1)**,** 1-11.

Nagase, H., Visse, R., and Murphy, G. (2006). Structure and function of matrix metalloproteinases and TIMPs. *Cardiovascular Research* 69**,** 11.

Nakagawa, T., Kubota, T., Kabuto, M., Sato, K., Kawano, H., Hayakawa, T., et al. (1994). Production of matrix metalloproteinases and tissue inhibitor of metalloproteinases-1 by human brain tumors. *Journal of Neurosurgery* 81(1)**,** 69-77.

Pagenstecher, A., Stalder, A., Kincaid, C., Shapiro, S., and Campbell, I. (1998). Differential expression of matrix metalloproteinase and tissue inhibitor of matrix metalloproteinase genes in the mouse central nervous system in normal and inflammatory states. *Am J Pathol* 152(3)**,** 729-741.

Parkitna, J., Korostynski, M., Kaminska-chowaniec, D., Obara, I., Mika, J., Przewlocka, B., et al. (2006). Comparison of gene expression profiles in neuropathic and inflammatory pain. *journal of pharmacology and physiology* 57(3)**,** 13.

Remacle, A., Hullugundi, S., Dolkas, J., Angert, M., Chernov, A., Strongin, A., et al. (2018). Acute- and late-phase matrix metalloproteinase (MMP)-9 activity is comparable in female and male rats after peripheral nerve injury. *Journal of Neuroinflammation* 15(89).

Ries, C. (2014). Cytokine functions of TIMP-1. *Cellular and Molcular Life Sciences* 71.

Tabachnick, B., and Fidell, L. (2007). *Using multivariate statistics.* Boston: Allyn & Bacon/Pearson Education.

Thorne, M., Moore, C., and Robertson, G. (2009). Lack of TIMP-1 increases severity of experimental autoimmune encephalomyelitis: Effects of darbepoetin alfa on TIMP-1 null and wild-type mice. *Journal of Neuroimmunology* 211(2009)**,** 8.

Treede, R., Meyer, R., Raja, S., and Campbell, J. (1992). Peripheral and central mechanisms of cutaneous hyperalgesia. *Progress in Neurobiology* 38**,** 24.

Treede, R., Rief, W., Barke, A., Aziz, Q., Bennett, M., Benoliel, R., et al. (2015). A classification of chronic pain for ICD-11. *Pain* 156(6)**,** 1003-1007.

Welser-Alves, J., Crocker, S., and Milner, R. (2011). A dual role for microglia in promoting tissue inhibitor of metalloproteinase (TIMP) expression in glial cells in response to neuroinflammatory stimuli. *Journal of Neuroinflammation* 8(61).

Yang, E., Bane, C., MacCallum, R., Kiecolt-Glaser, J., Malarkey, M., and Glaser, R. (2002). Stress-related modulation of matrix metalloproteinase expression. *Journal of Neuroimmunology* 133(2002)**,** 144-150.

Yokose, U., Hachiya, A., Sriwiriyanont, P., Fujimura, T., Visscher, M., Kitzmiller, W., et al. (2012). The endogenous protease inhibitor TIMP-1 mediates protection and recovery from cutaneous photodamage. *Journal of Investigative Dermatolology* 132(12). doi: 10.1038/jid.2012.204.